Journal of Organometallic Chemistry 695 (2010) 1155–1162

Contents lists available at ScienceDirect

Journal of Organometallic Chemistry

journal homepage: www.elsevier.com/locate/jorganchem

Magnesium, zinc, and calcium complexes based on tridentate nitrogen ligands: Syntheses, structures, and catalytic activities to the ring opening polymerization of *rac*-lactide

Xin Xu [a,b], Yaofeng Chen [b,*], Gang Zou [a,*], Zhi Ma [c], Guangyu Li [c]

[a] Laboratory of Advanced Materials and Institute of Fine Chemicals, East China University of Science and Technology, 130 Meilong Road, Shanghai 200237, PR China
[b] State Key Laboratory of Organometallic Chemistry, Shanghai Institute of Organic Chemistry, Chinese Academy of Sciences, 354 Fenglin Road, Shanghai 200032, PR China
[c] Analytical Laboratory, Shanghai Institute of Organic Chemistry, Chinese Academy of Sciences, 354 Fenglin Road, Shanghai 200032, PR China

ARTICLE INFO

Article history:
Received 3 December 2009
Received in revised form 12 January 2010
Accepted 19 January 2010
Available online 25 January 2010

Keywords:
Lactide
Ring-opening polymerization
Magnesium
Zinc
Calcium

ABSTRACT

A series of magnesium, zinc, and calcium monoalkyl or monoamide complexes containing tridentate nitrogen ligands, $CH_3C(2,6\text{-}(^iPr)_2C_6H_3N)CHC(CH_3)(NCH_2CH_2\text{–}D)$ (D = NMe_2, $N((CH_2CH_2)_2CH_2)$), have been synthesized, and six of which were characterized by single-crystal X-ray diffraction. The X-ray diffraction results show that the metal complexes are all solvent-free monomers and the pendant arm D bonds to the metal ion. These metal complexes are highly active for the ring-opening polymerization of *rac*-lactide and give preference for heterotactic polylactide.

1. Introduction

Polylactide (PLA) recently becomes one of the most important biodegradable polymers due to their biomedical and pharmaceutical application [1]. One method to synthesize PLA is the ring-opening polymerization (ROP) of lactide using metal complexes as the initiators [2–6]. Among these metal complexes, magnesium, zinc, and calcium complexes attracted great attention as these metal ions are biocompatible and environmentally friendly. Up to date, a number of such complexes containing various ancillary ligands, such as β-diketiminate [7–10], tris(pyrazolyl)hydroborate [11–13], phenolate [14–19], amino-bis(pyrazolyl) [20,21], and N-heterocyclic carbenes [22,23], have been synthesized, and their application for ROP of lactide have been studied. The research results show the metal complexes' ancillary ligands are crucial to molecular weight, molecular weight distribution, and microstructure of the PLA produced, which determine the polymer's mechanical and physical properties as well as biological degradation behaviors.

The β-diketiminato ligands play significant role in this class of complexes. Zinc complex supported by β-diketiminato ligand **A** (Chart 1) shows high activity and heterotactic selectivity for the polymerization of *rac*-lactide in CH_2Cl_2 and THF [7,24,25]. By contrast, its magnesium complex produces atactic PLA in CH_2Cl_2 and heterotactic PLA in THF [9,24,25]. Although the use of THF can increase the heterotactic selectivity, the complex's activity decreases due to THF competing with lactide for metal coordination. The aim to create a similar effect of THF led the development of the β-diketiminato derivatives, ligands **B** and **C** (Chart 1), which bear ether group. The magnesium, zinc, and calcium complexes of **B** and **C** were prepared, the complexes were active for the polymerization of lactide, and however, the stereoselectivity for heterotactic PLA was unsatisfied [26,27]. Ligands **B** and **C** both adopt rather rigid pendant arm, the interaction between metal ion and ether group is weak and easy to dissociate, which probably be the reason for low stereoselectivity in ROP of *rac*-lactide. Therefore, the changing of the pendant arm is needed. Recently, we designed a type of tridentate monoanionic ligands **D**, and prepared the precursors of **D** and their organolanthanide dialkyl complexes [28]. Contrast to **B** and **C**, **D** has a flexible pendant arm, and the interaction between the pendant amine group and the metal ion should be stronger. Thus we carried out the research on the syntheses and characterization of magnesium, zinc, and calcium complexes containing **D**, and the metal complexes' reactivities to ROP of *rac*-lactide. Herein, we would like to report these results.

* Corresponding authors. Tel.: +86 21 54925149; fax: +86 21 64166128.
E-mail addresses: yaofchen@sioc.ac.cn, yaofchen@mail.sioc.ac.cn (Y. Chen), zougang@ecust.edu.cn (G. Zou).

0022-328X/$ - see front matter
doi:10.1016/j.jorganchem.2010.01.023

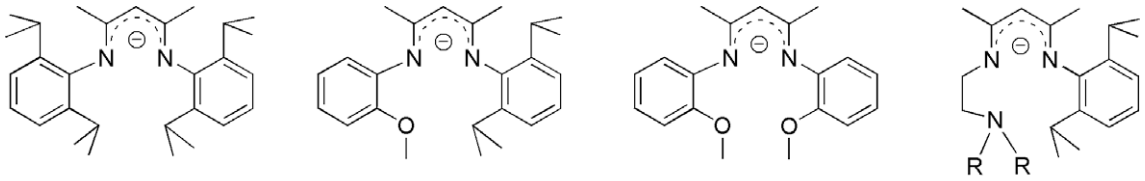

Chart 1.

2. Results and discussion

2.1. Syntheses and characterization of metal monoalkyl complexes

Ligand precursors, $CH_3C(2,6\text{-}(^iPr)_2C_6H_3NH)CHC(CH_3)(NCH_2\text{-}CH_2\text{–}D)$ (D = NMe_2 (**HL1**), $N((CH_2CH_2)_2CH_2)$ (**HL2**)), were prepared as we previously reported [28]. Magnesium and zinc monoalkyl complexes usually were synthesized through salt elimination or alkane elimination [29]. The latter was employed in our work as it is straightforward and the starting materials metal dialkyl complexes are commercially available. Addition of 1 equiv of $MgBu_2$ or $ZnEt_2$ to the ligand precursor, **HL1** or **HL2**, afforded the desired monoalkyl complexes, **1**, **2**, and **3**, in 87–92 % yield (Scheme 1). These were characterized by NMR (^1H, ^{13}C) and elemental analysis.

Single crystals of **1** and **2** were grown from concentrated hexane solutions at −35 °C and characterized by X-ray diffraction. ORTEP figures are shown in Fig. 1, and selected bond lengths and angles are listed in Table 1. Both complexes are solvent-free and four-coordinate monomers, the geometry at the metal centers can be better described as distorted tetrahedral. The ligand **L1** coordinates to the metal ion in a tridentate fashion. For the magnesium complex **1**, the pendant arm coordinates to the magnesium ion with a Mg–N3 distance of 2.28 Å. For the zinc complex **2**, a Zn–N3 distance of 2.46 Å was observed, this is significantly different from the reported zinc complexes with ligand **B** or **C**, where the oxygen atoms of ether groups are far from the metal centers [26,27]. The backbone of the ligand **L1** is bonded to the metal ion at Mg–N separations of 2.07 and 2.05 Å or Zn–N separations of 2.02 and 1.97 Å, which are close to those in the magnesium complexes with ligand **A** or **C** (2.05 Å (average)) and the zinc complexes with ligand **A**, **B** or **C** (1.95 Å (average)), respectively [8,25–27]. In both complexes, C–N and C–C bond lengths of the β-diketiminato backbone are intermediates between those of typical single and double bonds, and N1, C2, C3, C4, and N2 atoms are coplanar, indicating delocalized electronic structures. The metal ions lie 0.14 and 0.17 Å out of the β-diketiminato backbone C3N2 plane for **1** and **2**, respectively, which are slightly longer than those in magnesium butyl complex with ligand **A** (0.03 Å) and zinc ethyl complex with ligand **B** (0.04 Å). The M–C2, M–C3, and M–C4 distances (>2.93 Å) are too long for effective interaction. Thus, the bonding mode of β-diketiminato backbone is best described as 2-δ-electron donors.

2.2. Syntheses and characterization of metal monoamide complexes

Treatment of the magnesium alkyl complexes **1** and **3** with 1 equiv of $HN(SiMe_3)_2$ in toluene at room temperature provided the corresponding metal monoamide complexes **4** and **6** in high yields (81% for **4** and 94% for **6**, Scheme 2). However, the attempt to synthesize the zinc monoamide complex in this method failed, as the alkane elimination reaction of the zinc alkyl complex **2** with $HN(SiMe_3)_2$ did not occur even at the elevated temperature. The zinc monoamide complex **5** finally was synthesized by the reaction of the ligand precursor **HL1** with $Zn[N(SiMe_3)_2]_2$ in toluene (92% yield, Scheme 2). The synthesis of calcium monoamide complex supported by ligand **L1** was different from those of the magnesium and zinc analogues. Two equivalents of $KN(SiMe_3)_2$ and 1 equiv of ligand precursor **HL1** were mixed in THF, the addition of the mixture to a suspension of CaI_2 in THF gave the calcium monoamide complex **7** in 61% yield (Scheme 2). The complexes **4**, **5**, **6**, and **7** were characterized by NMR (^1H, ^{13}C) and elemental analysis.

Crystals of complexes **4**–**7** suitable for single-crystal X-ray crystallography were obtained from concentrated hexane solutions at −35 °C. ORTEP figures are shown in Figs. 2–5, selected bond lengths and angles are listed in Table 1. Similar to the monoalkyl complexes, the monoamide complexes are all solvent-free monomers. Interestingly, all the metal ions have coordination interaction with the neutral pendant arms (M–N3 2.29–2.53 Å) although the complexes have steric bulky amide groups. This does not happen in zinc complexes with ligand **B** or **C**. The backbone of the ligands bond to the metal ions at M - N separations from 1.97 to 2.34 Å, which fall in the range of 1.93–2.37 Å observed for M–N bonds in other reported β-diketiminato analogues, and the separation value increases with the size of metal ion. The structural data also show electronic delocalized backbones in the monoamide complexes. The M–N4 bond lengths vary from 1.93 to 2.30 Å according to the different metal ions, and these bond lengths are significantly shorter than M–N3 bond lengths (2.29–2.53 Å) due to different electronic donating property between N of the amide group and N of the pendant arm. The deviation values of the metal ions from the backbone C3N2 planes in these monoamide complexes are 0.27–0.44 Å, which are longer than those in the monalkyl complexes (0.14 and 0.17 Å). In the calcium complex **7**, the two Ca–N–Si angles, 110.5° and 119.8°, are non-equivalent, and the

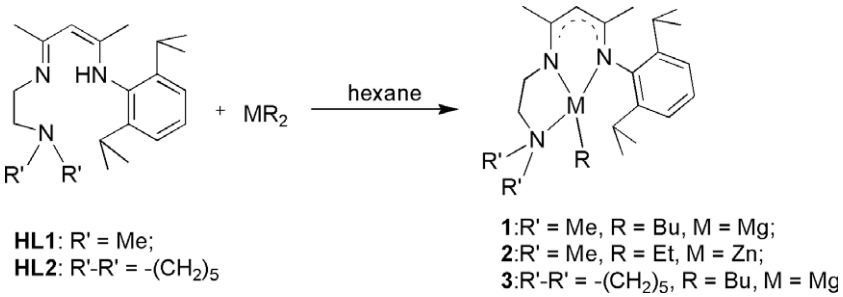

Scheme 1. Syntheses of magnesium and zinc monoalkyl complexes.

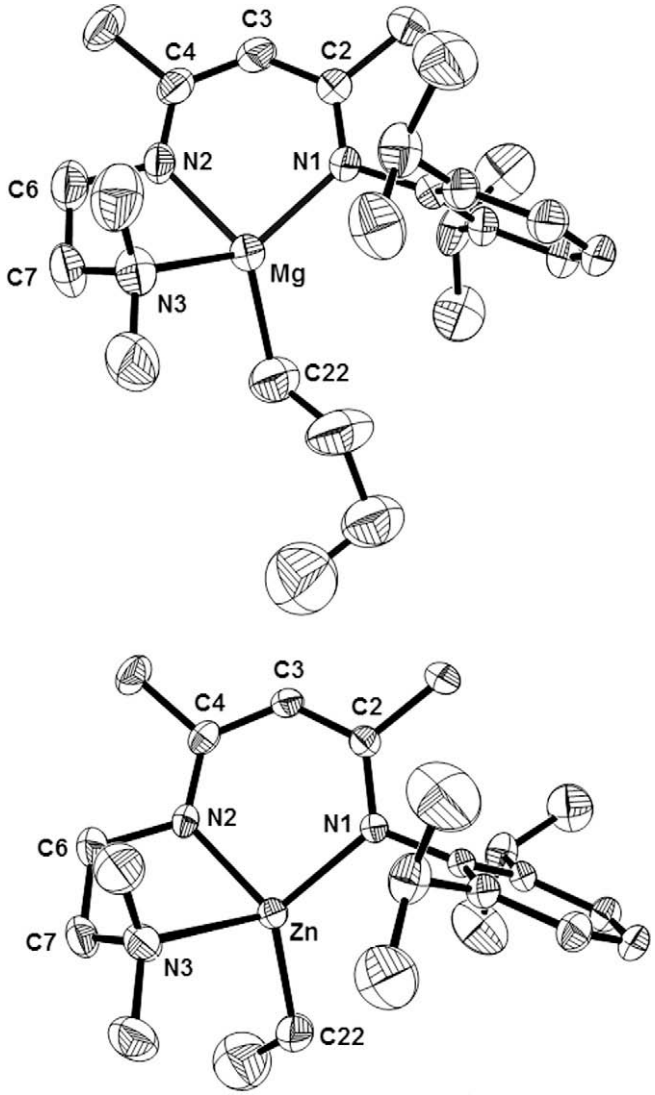

Fig. 1. Molecular structures of **1** and **2** with thermal ellipsoids at the 30% probability level. Hydrogen atoms are omitted for clarity.

Ca···C22 distance (3.11 Å) is significantly shorter than the Ca···C27 distance (3.52 Å). Similar observation was made in some other calcium amide complexes, and was ascribed to the agostic interaction between calcium ion and $-CH_3$ group [30–32].

2.3. Polymerization of rac-lactide

The complexes' reactivities toward the ring-opening polymerization of *rac*-lactide were studied, and the results are summarized in Table 2 [33,34]. The alkyl and amide complexes of magnesium (**1**, **3**, **4**, and **6**) all show high activities for the reaction in CH_2Cl_2 (entries 1, 3, 4, and 6), the monomer was nearly quantitatively converted into the polymer within 30 min by using 1 mol% of the metal complex as the initiator. Polymers produced by these magnesium complexes in CH_2Cl_2 show higher heterotactic bias ($P_r > 0.55$) than magnesium complexes with ligand **A** ($P_r = 0.37$), ligand **C** ($P_r = 0.49$) [27], indicating the effect from the pendant amine group's coordination. A related magnesium complex with ONN-tridentate ketiminato ligand was recently reported, interestingly, which catalyzed the ring-opening polymerization of *rac*-lactide to give a isotactic polymer ($P_m = 0.64$) [35]. The zinc amide complex **5** shows much higher activity than the zinc alkyl complex **2** (entry 5 vs. entry 2), that can be attributed to the slow initiation of the zinc alkyl complex [24]. The molecular weight distribution (M_w/M_n) of polymer provided by **5**, 1.07, is rather narrow, and M_n [33], 14 200, is very close to the calculated value based on the monomer/initiator ratio and conversion, 14 112. These observations are consistent with the characteristics of the living polymerization. The selectivity of these zinc complexes for heterotactic polymer in CH_2Cl_2 (0.69 and 0.68) are higher than that of the zinc complex bearing ligand **C** (0.59), and close to that of a related zinc complex bearing ONN-tridentate ketiminato ligand (0.70) [35]. Compared to the corresponding metal complexes with ligand **A**, the magnesium complexes are less active while the zinc complexes are more active. These are probably due to the coordination strength between the pendant arm and the metal ion, the interaction between the pendant amine group and the magnesium ion is stronger than that with zinc ion. The activity of the calcium amide complex **7** in CH_2Cl_2 is also high, but the selectivity is low, 0.47 (entry 7). When the polymerization was proceeded in THF, the magnesium amide **6** gave a polymer with a higher heterotactic bias, 0.75 (entry 9), which is probably due to that the ligand **L2** is not enough sterically bulky and the THF coordinates to the metal center and promotes the stereoselectivity. The solvent effect in the complex **6** catalyzed polymerization is not as distinguish as that in the magnesium complex with ligand **A** or the magnesium complex with ONN-tridentate ketiminato ligand catalyzed polymerization, which

Table 1
Selected bond lengths (Å) and angles (°) for complexes **1, 2,** and **4**–**7**.

	1 (M = Mg)	**2** (M = Zn)	**4** (M = Mg)	**5** (M = Zn)	**6** (M = Mg)	**7** (M = Ca)
M–N1	2.066(2)	2.016(2)	2.067(2)	2.0061(19)	2.0773(18)	2.344(4)
M–N2	2.047(3)	1.974(2)	2.029(2)	1.973(2)	2.0455(19)	2.348(4)
M–N3	2.282(3)	2.457(3)	2.291(2)	2.362(2)	2.304(2)	2.527(4)
M–N4			2.007(2)	1.9315(19)	2.0213(19)	2.303(4)
M–C22	2.135(4)	1.983(3)				
C2–N1	1.329(3)	1.330(3)	1.330(3)	1.327(3)	1.337(3)	1.321(5)
C4–N2	1.318(4)	1.320(4)	1.318(3)	1.318(3)	1.308(3)	1.310(5)
C2–C3	1.400(3)	1.395(4)	1.401(4)	1.394(3)	1.386(3)	1.408(6)
C3–C4	1.387(4)	1.386(4)	1.396(4)	1.392(4)	1.403(3)	1.404(7)
N_2C_3–M	0.145(3)	0.171(3)	0.353(3)	0.344(2)	0.277(2)	0.437(6)
N1–M–N2	90.47(10)	94.91(9)	91.32(9)	95.41(8)	90.54(8)	78.42(14)
N1–M–N3	132.47(10)	123.16(9)	128.76(9)	125.29(8)	128.90(8)	132.53(14)
N2–M–N3	77.88(11)	74.41(9)	77.28(9)	76.35(8)	76.90(7)	71.90(15)
N1–C2–C3	124.1(3)	124.5(3)	124.8(2)	124.4(2)	124.6(2)	123.3(4)
C2–C3–C4	129.5(3)	129.9(3)	129.6(2)	130.4(2)	129.8(2)	130.1(4)
C3–C4–N2	123.0(3)	123.4(3)	122.5(2)	122.8(2)	122.6(2)	124.1(5)
M–N1–C2	125.00(18)	121.90(18)	122.81(17)	120.83(17)	123.64(14)	130.8(3)
M–N2–C4	127.05(19)	124.5(2)	126.16(18)	123.37(18)	127.04(16)	129.5(3)
M–N3–C7	92.7(2)	90.43(18)	94.69(16)	93.20(15)	93.50(14)	94.1(3)

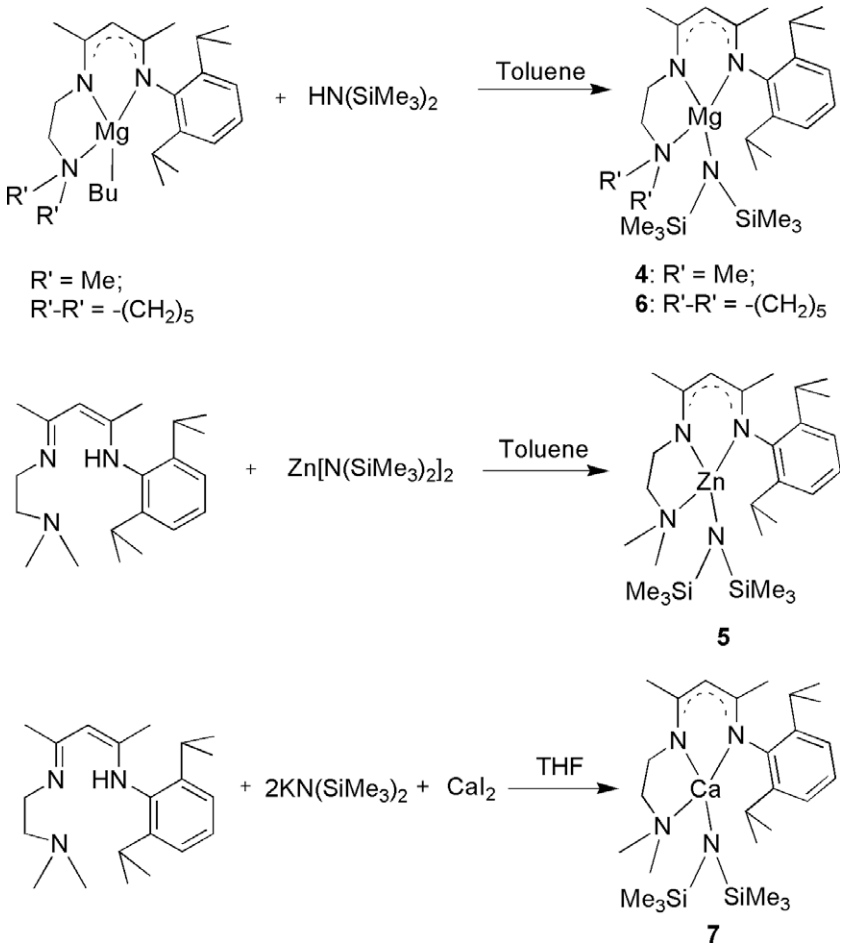

Scheme 2. Syntheses of magnesium, zinc, and calcium monoamide complexes.

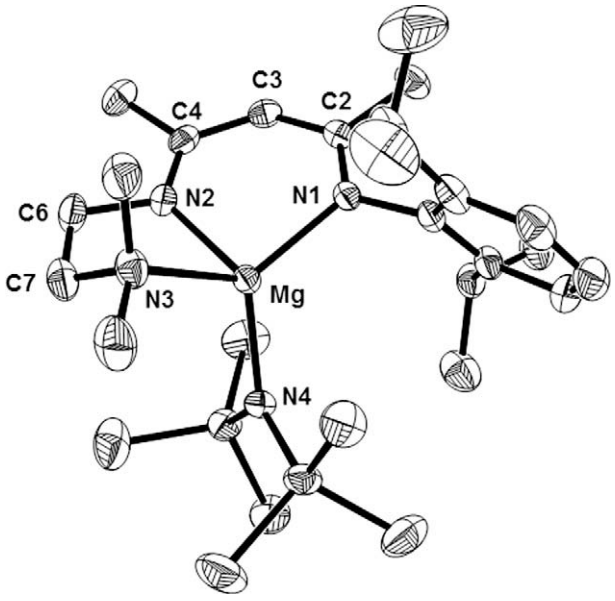

Fig. 2. Molecular structure of **4** with thermal ellipsoids at the 30% probability level. Hydrogen atoms are omitted for clarity.

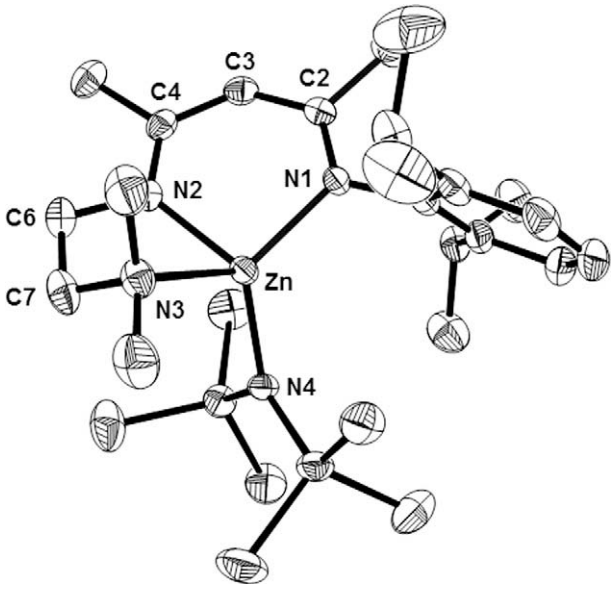

Fig. 3. Molecular structure of **5** with thermal ellipsoids at the 30% probability level. Hydrogen atoms are omitted for clarity.

gives much higher heterotactic selectivity in THF than in CH_2Cl_2 [25,35]. A higher heterotactic selectivity was also observed for the calcium complex **7** in THF in comparison to that in CH_2Cl_2, entry 10 vs. entry 7, but at a price of much lower activity. For the zinc complex **5**, the solvent effect on the polymerization is little, entry 5 vs. entry 8.

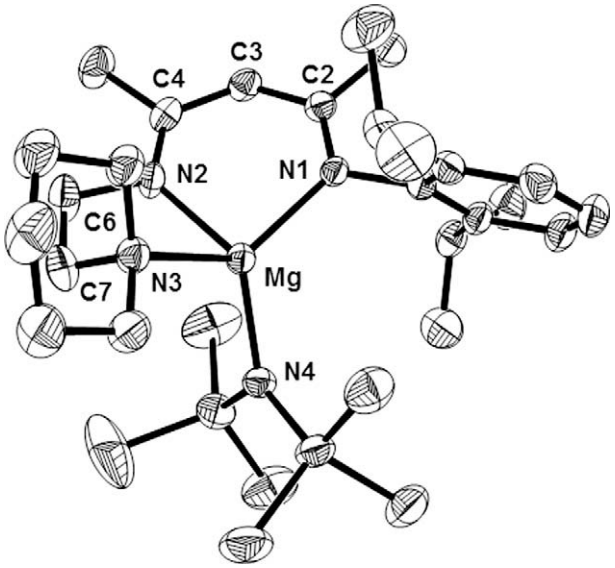

Fig. 4. Molecular structure of **6** with thermal ellipsoids at the 30% probability level. Hydrogen atoms are omitted for clarity.

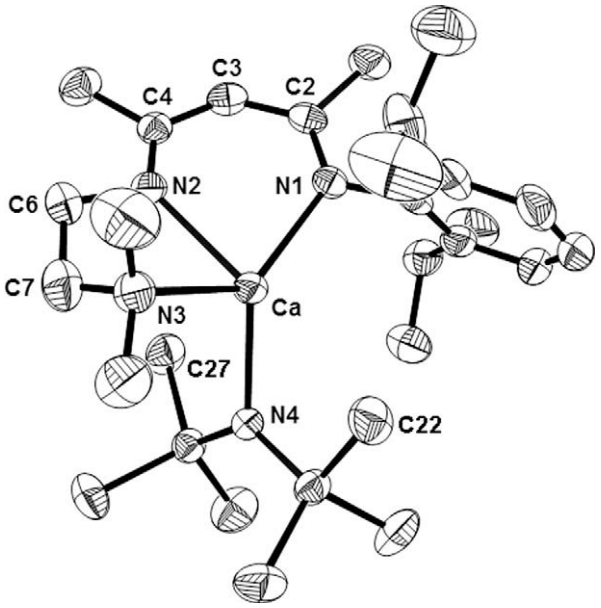

Fig. 5. Molecular structure of **7** with thermal ellipsoids at the 30% probability level. Hydrogen atoms are omitted for clarity.

3. Conclusion

The alkane elimination of $ZnEt_2$ or $MgBu_2$ with tridentate nitrogen ligand precursors, $CH_3C(2,6\text{-}(^iPr)_2C_6H_3NH)CHC(CH_3)$ (NCH_2-CH_2–D) (D = NMe_2, $N((CH_2CH_2)_2CH_2)$), provided the corresponding zinc and magnesium monoalkyl complexes in high yield. Treatment of the above magnesium monoalkyl complexes with 1 equiv. of $HN(SiMe_3)_2$ successfully generated the magnesium monoamide complexes, while that for the zinc complex failed. The zinc monoamide complex was finally obtained through the amine elimination reaction of $Zn[N(SiMe_3)_2]_2$ with the ligand precursor. The reactions of $KN(SiMe_3)_2$, ligand precursor, and CaI_2 produced the calcium monoamide complex. The flexibility of the pendant arm and the strong electronic donating property of the nitrogen atom benefit the coordination interaction between the metal ion and the nitrogen atom on the pendant arm. The complexes are active to the ROP of *rac*-lactide, the catalytic activities of the complexes, molecular weight distribution and microstructure of polymers produced were influenced by the metal ion, initiating group, and solvent. The magnesium complexes gave polymers with higher heterotactic bias in CH_2Cl_2 in comparison to other reported analogues, showing the effect from the pendant amine group's coordination.

4. Experimental

4.1. General

All operations were carried out under an atmosphere of argon using standard Schlenk techniques or in a nitrogen gas filled glovebox. Toluene, hexane, and C_6D_6 were dried over Na/K alloy, distilled under vacuum, and stored in the glovebox. THF was distilled from Na-benzophenone ketyl under nitrogen. CH_2Cl_2 was dried over CaH_2, and distilled under nitrogen. $CDCl_3$ was dried over 4 Å molecular sieves. $HN(SiMe_3)_2$ was dried over CaH_2, distilled and degassed prior to use. $KN(SiMe_3)_2$ [36] and $Zn[N(SiMe_3)_2]_2$ [37] were prepared according to the literatures. Ligands precursors, **HL1** and **HL2**, were synthesized following the published procedures [28]. *rac*-Lactide was purified by sublimation three times, and then recrystallization from dry ethyl acetate. ^1H and ^{13}C NMR spectra were recorded on a Varian Mercury 300 or 400 spectrometers, and the chemical shifts were reported in δ (ppm) units with references to the residual solvent resonance of the deuterated solvents. Gel permeation chromatographic analysis was performed on a Waters 1515 apparatus equipped with a set of Waters Styragel columns (HR3, HR4 and HR5) at 35 °C. THF was used as the eluent, and the system was calibrated using polystyrene standards. Elemental analysis was performed by Analytical Laboratory of Shanghai Institute of Organic Chemistry. Melting points of the complexes were determined on a Digital Melting Point Apparatus SWG X-4 in a sealed capillary and are uncorrected.

4.2. Synthesis of L1MgBu (**1**)

$MgBu_2$ (2.0 mL, 1.0 M in heptane, 2.0 mmol) was added to a solution of **HL1** (659 mg, 2.0 mmol) in 6 mL of hexane at −35 °C. After stirring at room temperature for 24 h, the reaction mixture was concentrated to approximately 2 mL and cooled to −35 °C to give **1** as a pale red crystalline solid (716 mg, 87% yield). Mp: 87–89 °C. Anal. Calc. for $C_{25}H_{43}N_3Mg$: C, 73.25; H, 10.57; N, 10.25. Found: C, 72.72; H, 10.44; N, 10.38%. ^1H NMR (300 MHz, C_6D_6, 25 °C): δ (ppm) 7.16 (m, 3H, Ar*H*), 4.76 (s, 1H, MeC(N)C*H*), 3.28 (sp, $^3J_{HH}$ = 6.9 Hz, 2H, ArC*H*Me_2), 2.83 (t, $^3J_{HH}$ = 6.3 Hz, 2H, NCH_2), 2.20 (t, $^3J_{HH}$ = 6.3 Hz, 2H, NCH_2), 1.82 (s, 6H, NMe_2), 1.70 (s, 3H, *Me*C), 1.69 (s, 3H, *Me*C), 1.63–1.53 (m, 4H, $MgCH_2(CH_2)_2CH_3$), 1.32 (d, $^3J_{HH}$ = 6.6 Hz, 6H, ArCHMe_2), 1.19 (d, $^3J_{HH}$ = 6.6 Hz, 6H, ArCHMe_2), 1.22 (t, $^3J_{HH}$ = 6.9 Hz, 3H, $Mg(CH_2)_3CH_3$), −0.19 (t, $^3J_{HH}$ = 7.5 Hz, 2H, $MgCH_2(CH_2)_2CH_3$). ^{13}C NMR (75 MHz, C_6D_6, 25 °C): δ (ppm) 168.4 (imine-*C*), 166.7 (imine-*C*), 146.4, 142.3, 124.9, 123.8 (Ar*C*), 94.9 (MeC(N)CH), 56.8 (NCH_2), 44.5 (NCH_2), 43.9 (NMe_2), 33.1 ($MgCH_2(CH_2)_2CH_3$), 32.5 ($MgCH_2(CH_2)_2CH_3$), 28.2 (ArCHMe_2), 24.8 (ArCHMe_2), 24.4 (ArCHMe_2), 23.9 (*Me*C), 21.8 (*Me*C), 14.6 ($Mg(CH_2)_3CH_3$), 7.8 ($MgCH_2$).

4.3. Synthesis of L1ZnEt (**2**)

Following the procedure described for **1**, reaction of $ZnEt_2$ (2.0 mL, 1.0 M in hexane, 2.0 mmol) and **HL1** (659 mg, 2.0 mmol) gave **2** as a pale yellow crystalline solid (776 mg, 92% yield). Mp: 67–69 °C. Anal. Calc. for $C_{23}H_{39}N_3Zn$: C, 65.31; H, 9.29; N, 9.93. Found: C, 64.89; H, 8.91; N, 9.83%. ^1H NMR (300 MHz, C_6D_6,

Table 2
Polymerization of *rac*-lactide with complexes **1**–**7**.[a]

Entry	Initiator	Time (min)	Solvent	Conversion[b] (%)	M_n[c]	M_w/M_n[d]	P_r[e]
1	**1**	30	CH_2Cl_2	98	18 700	1.37	0.55
2	**2**	120	CH_2Cl_2	96	15 000	1.20	0.69
3	**3**	30	CH_2Cl_2	98	20 500	1.26	0.55
4	**4**	30	CH_2Cl_2	98	17 200	1.72	0.55
5	**5**	30	CH_2Cl_2	98	14 200	1.07	0.68
6	**6**	30	CH_2Cl_2	98	14 900	1.43	0.57
7	**7**	30	CH_2Cl_2	90	22 400	1.34	0.47
8	**5**	30	THF	98	15 700	1.18	0.67
9	**6**	30	THF	98	18 800	1.40	0.75
10	**7**	120	THF	66	13 200	1.26	0.56

[a] [LA]/[initiator] = 100, T = 25 °C.
[b] Monomer conversion determined by ^{1}H NMR spectroscopy.
[c] Determined by GPC relative to polystyrene standards and corrected by a coefficient of 0.58 [33].
[d] Determined by GPC.
[e] P_r is the probability of heterotactic enchainment determined by homonuclear decoupled ^{1}H NMR spectroscopy [24,34].

25 °C): δ (ppm) 7.16 (m, 3H, Ar*H*), 4.78 (s, 1H, MeC(N)C*H*), 3.20 (m, 4H, ArC*H*Me$_2$ and NC*H*$_2$), 2.26 (t, $^3J_{HH}$ = 6.6 Hz, 2H, NC*H*$_2$), 1.99 (s, 6H, N*Me*$_2$), 1.77 (s, 3H, *Me*C), 1.69 (s, 3H, *Me*C), 1.28 (d, $^3J_{HH}$ = 6.6 Hz, 6H, ArCH*Me*$_2$), 1.25 (t, $^3J_{HH}$ = 8.4 Hz, 3H, ZnCH$_2$C*H*$_3$), 1.18 (d, $^3J_{HH}$ = 6.6 Hz, 6H, ArCH*Me*$_2$), 0.42 (q, $^3J_{HH}$ = 8.4 Hz, 2H, ZnC*H*$_2$CH$_3$). ^{13}C NMR (75 MHz, C_6D_6, 25 °C): δ (ppm) 167.3 (imine-*C*), 165.5 (imine-*C*), 146.3, 141.8, 125.3, 123.6 (Ar*C*), 95.2 (MeC(N)*C*H), 59.3 (NCH$_2$), 47.7 (NCH$_2$), 44.9 (N*Me*$_2$), 28.2 (Ar*C*HMe$_2$), 24.3 (ArCH*Me*$_2$), 23.9 (ArCH*Me*$_2$), 23.2 (*Me*C), 22.1 (*Me*C), 12.9 (ZnCH$_2$*C*H$_3$), −0.6 (Zn*C*H$_2$CH$_3$).

4.4. Synthesis of L2MgBu (**3**)

Following the procedure described for **1**, reaction of MgBu$_2$ (1.0 mL, 1.0 M in heptane, 1.0 mmol) and **HL2** (369 mg, 1.0 mmol) gave **3** as a pale red crystalline solid (413 mg, 92% yield). Mp: 94–96 °C. Anal. Calc. for $C_{28}H_{47}N_3Mg$: C, 74.73; H, 10.53; N, 9.34. Found: C, 75.60; H, 10.89; N, 9.47%. ^{1}H NMR (300 MHz, C_6D_6, 25 °C): δ (ppm) 7.16 (m, 3H, Ar*H*), 4.81 (s, 1H, MeC(N)C*H*), 3.41 (sp, $^3J_{HH}$ = 6.9 Hz, 2H, ArC*H*Me$_2$), 2.92 (t, $^3J_{HH}$ = 6.0 Hz, 2H, NC*H*$_2$), 2.31 (br, 2H, NC*H*$_2$), 1.74 (s, 3H, *Me*C), 1.71 (s, 3H, *Me*C), 1.64–1.56 (m, 4H, MgCH$_2$(C*H*$_2$)$_2$CH$_3$), 1.36 (d, $^3J_{HH}$ = 6.6 Hz, 6H, ArCH*Me*$_2$), 1.26 (m, 6H, N(CH$_2$C*H*$_2$)$_2$CH$_2$ and N(CH$_2$CH$_2$)$_2$C*H*$_2$), 1.24 (d, $^3J_{HH}$ = 6.6 Hz, 6H, ArCH*Me*$_2$), 1.15 (t, $^3J_{HH}$ = 6.9 Hz, 3H, Mg(CH$_2$)$_3$C*H*$_3$), −0.15 (t, $^3J_{HH}$ = 7.2 Hz, 2H, MgC*H*$_2$(CH$_2$)$_2$CH$_3$). ^{13}C NMR (75 MHz, C_6D_6, 25 °C): δ (ppm) 168.1 (imine-*C*), 167.1 (imine-*C*), 147.2, 142.5, 124.7, 123.8 (Ar*C*), 95.5 (MeC(N)*C*H), 56.4 (NCH$_2$), 53.2 (NCH$_2$), 43.6 (N(*C*H$_2$CH$_2$)$_2$CH$_2$), 33.3 (MgCH$_2$-(*C*H$_2$)$_2$CH$_3$), 32.3 (MgCH$_2$(CH$_2$)$_2$CH$_3$), 28.4 (Ar*C*HMe$_2$), 25.8 (ArCH*Me*$_2$), 24.8 (N(CH$_2$*C*H$_2$)$_2$CH$_2$), 24.7 (ArCH*Me*$_2$), 24.5 (N(CH$_2$-*C*H$_2$)$_2$CH$_2$), 23.9 (*Me*C), 21.5 (*Me*C), 14.7 (Mg(CH$_2$)$_3$*C*H$_3$), 8.5 (Mg*C*H$_2$).

4.5. Synthesis of L1MgN(SiMe$_3$)$_2$ (**4**)

HN(SiMe$_3$)$_2$ (130 mg, 0.80 mmol) was added to a solution of complex **1** (300 mg, 0.73 mmol) in 8 mL of toluene at room temperature. After stirring for 36 h, the volatiles were removed under vacuum and the solid residue was recrystallized in 2 mL of hexane at −35 °C to afford **4** as a pale red crystalline solid (303 mg, 81% yield). Mp: 245–248 °C. Anal. Calc. for $C_{27}H_{52}N_4Si_2Mg$: C, 63.19; H, 10.21; N, 10.92. Found: C, 63.14; H, 9.84; N, 10.73%. ^{1}H NMR (300 MHz, C_6D_6, 25 °C): δ (ppm) 7.16 (m, 3H, Ar*H*), 4.77 (s, 1H, MeC(N)C*H*), 3.13 (br, 2H, ArC*H*Me$_2$), 2.97 (br, 2H, NC*H*$_2$), 1.94 (s, 6H, N*Me*$_2$), 1.71 (s, 3H, *Me*C), 1.69 (s, 3H, *Me*C), 1.42 (br, 6H, ArCH*Me*$_2$), 1.15 (d, $^3J_{HH}$ = 6.6 Hz, 6H, ArCH*Me*$_2$), 0.18 (s, 18H, Si*Me*$_3$). ^{13}C NMR (75 MHz, C_6D_6, 25 °C): δ (ppm) 168.5 (imine-*C*), 167.8 (imine-*C*), 146.5, 142.1, 125.1, 123.8 (Ar*C*), 95.0 (MeC(N)*C*H), 57.8 (NCH$_2$), 44.1 (N*Me*$_2$), 28.4 (ArCHMe$_2$), 24.5 (ArCH*Me*$_2$), 24.4 (*Me*C), 21.9 (*Me*C), 6.1 (Si*Me*$_3$).

4.6. Synthesis of L1ZnN(SiMe$_3$)$_2$ (**5**)

A solution of Zn[N(SiMe$_3$)$_2$]$_2$ (425 mg, 1.1 mmol in 3 mL of toluene) was added to a solution of **HL1** (330 mg, 1.0 mmol) in 5 mL of toluene at room temperature. After stirring for 24 h, the volatiles were removed under vacuum and the solid residue was recrystallized in 2 mL of hexane at −35 °C to afford **5** as pale yellow crystals (512 mg, 92% yield). Mp: 119–121 °C. Anal. Calc. for $C_{27}H_{52}N_4Si_2Zn$: C, 58.51; H, 9.46; N, 10.11. Found: C, 58.86; H, 10.14; N, 9.89%. ^{1}H NMR (400 MHz, C_6D_6, 25 °C): δ (ppm) 7.15 (m, 3H, Ar*H*), 4.67 (s, 1H, MeC(N)C*H*), 3.30 (t, $^3J_{HH}$ = 6.6 Hz, 2H, NC*H*$_2$), 3.19 (sp, $^3J_{HH}$ = 6.8 Hz, 2H, ArC*H*Me$_2$), 2.36 (t, $^3J_{HH}$ = 6.4 Hz, 2H, NC*H*$_2$), 2.05 (s, 6H, N*Me*$_2$), 1.69 (s, 3H, *Me*C), 1.65 (s, 3H, *Me*C), 1.39 (d, $^3J_{HH}$ = 6.8 Hz, 6H, ArCH*Me*$_2$), 1.12 (d, $^3J_{HH}$ = 6.8 Hz, 6H, ArCH*Me*$_2$), 0.18 (s, 18H, Si*Me*$_3$). ^{13}C NMR (100 MHz, C_6D_6, 25 °C): δ (ppm) 168.1 (imine-*C*), 167.2 (imine-*C*), 145.7, 142.3, 125.7, 123.9 (Ar*C*), 94.9 (MeC(N)*C*H), 59.8 (NCH$_2$), 46.6 (NCH$_2$), 45.9 (N*Me*$_2$), 28.3 (Ar*C*HMe$_2$), 24.8 (ArCH*Me*$_2$), 24.4 (ArCH*Me*$_2$), 24.2 (*Me*C), 21.9 (*Me*C), 5.8 (Si*Me*$_3$).

4.7. Synthesis of L2MgN(SiMe$_3$)$_2$ (**6**)

Following the procedure described for **4**, reaction of HN(SiMe$_3$)$_2$ (130 mg, 0.80 mmol) and complex **3** (328 mg, 0.73 mmol) gave **6** as a pale red crystalline solid (379 mg, 94% yield). Mp: 143–145 °C. Anal. Calc. for $C_{30}H_{56}N_4Si_2Mg$: C, 65.13; H, 10.20; N, 10.13. Found: C, 66.18; H, 10.38; N, 10.00%. The higher carbon content found is due to the remaining of small amount of hexane, which is hard to be completely removed under vacuum. ^{1}H NMR (400 MHz, C_6D_6, 25 °C): δ (ppm) 7.16 (m, 3H, Ar*H*), 4.76 (s, 1H, MeC(N)C*H*), 3.23 (sp, $^3J_{HH}$ = 6.8 Hz, 2H, ArC*H*Me$_2$), 3.08 (t, $^3J_{HH}$ = 6.4 Hz, 2H, NC*H*$_2$), 2.86 (t, $^3J_{HH}$ = 6.4 Hz, 2H, NC*H*$_2$), 2.69 (br, 4H, N(C*H*$_2$CH$_2$)$_2$CH$_2$), 1.71 (s, 3H, *Me*C), 1.70 (s, 3H, *Me*C), 1.45 (d, $^3J_{HH}$ = 6.4 Hz, 6H, ArCH*Me*$_2$), 1.16 (d, $^3J_{HH}$ = 6.4 Hz, 6H, ArCH*Me*$_2$), 1.19–1.12 (m, 6H, N(CH$_2$C*H*$_2$)$_2$CH$_2$ and N(CH$_2$CH$_2$)$_2$C*H*$_2$), 0.18 (s, 18H, Si*Me*$_3$). ^{13}C NMR (100 MHz, C_6D_6, 25 °C): δ (ppm) 168.5 (imine-*C*), 167.9 (imine-*C*), 146.8, 142.3, 125.2, 123.9 (Ar*C*), 94.9 (MeC(N)*C*H), 51.4 (NCH$_2$), 48.3 (NCH$_2$), 43.7 (N(*C*H$_2$CH$_2$)$_2$CH$_2$), 28.5 (ArCHMe$_2$), 25.1 (ArCH*Me*$_2$), 24.7 (N(CH$_2$*C*H$_2$)$_2$CH$_2$), 24.6 (ArCH*Me*$_2$), 24.4 (N(CH$_2$CH$_2$)$_2$*C*H$_2$), 21.9 (*Me*C), 19.9 (*Me*C), 6.2 (Si*Me*$_3$).

Table 3
Crystallographic data and refinement for complexes **1, 2,** and **4–7**.

	1	2	4	5	6	7
Formula	$C_{25}H_{43}N_3Mg$	$C_{23}H_{39}N_3Zn$	$C_{27}H_{52}N_4Si_2Mg$	$C_{27}H_{52}N_4Si_2Zn$	$C_{30}H_{56}N_4Si_2Mg$	$C_{27}H_{52}N_4Si_2Ca$
Formula weight	409.93	422.94	513.22	554.28	553.28	528.99
Color	colorless	pale yellow	colorless	colorless	colorless	pale yellow
Crystal system	monoclinic	monoclinic	monoclinic	monoclinic	monoclinic	monoclinic
Space group	*P*2(1)/*n*	*P*2(1)/*n*	*P*2(1)/*c*	*P*2(1)/*c*	*P*2(1)/*c*	*P*2(1)/*n*
a (Å)	9.6584(11)	8.7133(10)	16.8493(14)	16.8413(15)	9.1760(7)	8.858(4)
b (Å)	18.3912(19)	18.944(2)	10.3135(9)	10.2723(9)	20.1685(15)	24.977(11)
c (Å)	15.1579(16)	14.8785(16)	19.2601(16)	19.1934(17)	18.8794(14)	15.061(7)
β (°)	98.601(2)	102.069(2)	105.193(2)	105.103(2)	96.194(2)	93.725(10)
V (Å^3)	2662.2(5)	2401.7(5)	3229.9(5)	3205.7(5)	3473.5(5)	3325(3)
Z	4	4	4	4	4	4
D_{calc} (g/cm^3)	1.023	1.170	1.055	1.148	1.058	1.057
F(0 0 0)	904	912	1128	1200	1216	1160
θ (°)	2.21–26.00	1.76–27.00	1.25–27.00	2.20–27.00	2.02–26.50	1.58–27.00
Reflections collected	14 391	13 940	18 538	18 433	19 644	19 476
Number of unique reflections	5209	5211	7026	6905	7149	7259
Number of observed reflections ($I > 2\sigma(I)$)	2005	3291	4416	4916	4115	2302
Number of parameters	264	248	321	322	346	321
Goodness-of-fit (GOF)	0.810	0.925	0.983	0.944	0.910	0.917
Final *R* indicates $R_w(I > 2\sigma(I))$	0.0567, 0.1346	0.0482, 0.1170	0.0629, 0.1433	0.0453, 0.0994	0.0563, 0.1219	0.0643, 0.1413
$\Delta\rho_{max,\ min}$ (eÅ^{-3})	0.277, −0.173	0.751, −0.425	0.302, −0.202	0.762, −0.346	0.253, −0.190	0.324, −0.323

4.8. Synthesis of L1CaN(SiMe$_3$)$_2$ (7)

HL1 (330 mg, 1.0 mmol) and KN(SiMe$_3$)$_2$ (399 mg, 2.0 mmol) were mixed in 25 mL of THF at room temperature. After stirring for 1 h, the reaction mixture was added to a slurry of CaI_2 (323 mg, 1.1 mmol) in 8 mL of THF and stirred overnight. The volatiles were removed under vacuum and the solid residue was extracted with 20 mL of hexane. Concentration of the extract solution in vacuo to approximately 5 mL and cooling to −35 °C afford **7** as a pale yellow crystalline solid (325 mg, 61% yield). Mp: 213–215 °C. Anal. Calc. for $C_{27}H_{52}N_4Si_2Ca$: C, 61.30; H, 9.91; N, 10.59. Found: C, 61.67; H, 9.46; N, 10.20%. ^{1}H NMR (300 MHz, C_6D_6, 25 °C): δ (ppm) 7.14–7.12 (m, 3H, Ar*H*), 4.75 (s, 1H, MeC(N)-C*H*), 3.17 (sp, $^3J_{HH}$ = 6.9 Hz, 2H, ArC*H*Me$_2$), 3.02 (t, $^3J_{HH}$ = 6.3 Hz, 2H, NC*H*$_2$), 2.42 (t, $^3J_{HH}$ = 6.3 Hz, 2H, NC*H*$_2$), 1.92 (s, 6H, N*Me*$_2$), 1.77 (s, 3H, *Me*C), 1.73 (s, 3H, *Me*C), 1.34 (d, $^3J_{HH}$ = 6.9 Hz, 6H, ArCH*Me*$_2$), 1.14 (d, $^3J_{HH}$ = 6.9 Hz, 6H, ArCH*Me*$_2$), 0.13 (s, 18H, Si*Me*$_3$). ^{13}C NMR (75 MHz, C_6D_6, 25 °C): δ (ppm) 167.2 (imine-*C*), 163.9 (imine-*C*), 145.2, 141.9, 124.7, 124.3 (Ar*C*), 95.1 (MeC(N)*C*H), 58.6 (NCH$_2$), 46.4 (NCH$_2$), 44.8 (N*Me*$_2$), 28.3 (ArCHMe$_2$), 25.3 (ArCH*Me*$_2$), 24.4 (ArCH*Me*$_2$), 23.5 (*Me*C), 22.6 (*Me*C), 5.1 (Si*Me*$_3$).

4.9. General polymerization procedure

The metal complex (19.5 μmol) and *rac*-lactide (281 mg, 1.95 mmol) were mixed in 2 mL of CH_2Cl_2 or THF. After a certain time, the polymerization was quenched with a drop of wet THF and all the volatiles were removed under vacuum. The monomer conversions were determined by ^{1}H NMR analysis of the residues in $CDCl_3$. The residues were dissolved in CH_2Cl_2, and excess of cold methanol was added to the above solution. Polymers precipitated were collected and dried under vacuum to constant weight.

4.10. X-ray crystallography

Suitable single crystals of **1**, **2**, and **4–7** were sealed in thin-walled glass capillaries, and data collection was performed at 20 °C on a Bruker SMART diffractometer with graphite-monochromated Mo Kα radiation (λ = 0.71073 Å). The SMART program package was used to determine the unit-cell parameters. The absorption correction was applied using SADABS. The structures were solved by direct methods and refined on F^2 by full-matrix least squares techniques with anisotropic thermal parameters for non-hydrogen atoms. Hydrogen atoms were placed at calculated positions and were included in the structure calculation without further refinement of the parameters. All calculations were carried out using the SHELXS-97 program. The software used is listed in the Refs. [38–42] Crystallographic data and refinement for **1**, **2**, and **4–7** are listed in Table 3.

Acknowledgment

This work was supported by the National Natural Science Foundation of China (Grant Nos. 20672134, 20872164 and 20821002), Chinese Academy of Sciences and Shanghai Municipal Committee of Science and Technology (Grant No. 07JC14063).

Appendix A. Supplementary material

CCDC 756109–756114 contain X-ray crystallographic data for **1**, **2**, and **4–7**. This material is available free of charge from the Cambridge Crystallographic Data Centre via www.ccdc.cam.ac.uk/data_request/cif. Supplementary data associated with this article can be found, in the online version, at doi:10.1016/j.jorganchem.2010.01.023.

References

[1] R.E. Drumright, P.R. Gruber, D.E. Henton, Adv. Mater. 12 (2000) 1841–1846.
[2] B.J. O'Keefe, M.A. Hillmyer, W.B. Tolman, J. Chem. Soc., Dalton Trans. (2001) 2215–2224.
[3] O. Dechy-Cabaret, B. Martin-Vaca, D. Bourissou, Chem. Rev. 104 (2004) 6147–6176.
[4] J. Wu, T.L. Yu, C.T. Chen, C.C. Lin, Coord. Chem. Rev. 250 (2006) 602–626.
[5] C.A. Wheaton, P.G. Hayes, B.J. Ireland, Dalton Trans. (2009) 4832–4846.
[6] Y.L. Ning, Y.T. Zhang, A. Delgado-Rodriguez, E.Y.-X. Chen, Organometallics 27 (2008) 5632–5640.
[7] M. Cheng, A.B. Attygalle, E.B. Lobkovsky, G.W. Coates, J. Am. Chem. Soc. 121 (1999) 11583–11584.
[8] V.C. Gibson, J.A. Segal, A.J.P. White, D.J. Williams, J. Am. Chem. Soc. 122 (2000) 7120–7121.
[9] M.H. Chisholm, J.C. Huffman, K. Phomphrai, J. Chem. Soc., Dalton Trans. (2001) 222–224.
[10] L.F. Sánchez-Barba, D.L. Hughes, S.M. Humphrey, M. Bochmann, Organometallics 25 (2006) 1012–1020.
[11] M.H. Chisholm, N.W. Eilerts, J.C. Huffman, S.S. Iyer, M. Pacold, K. Phomphrai, J. Am. Chem. Soc. 122 (2000) 11845–11854.
[12] M.H. Chisholm, J. Gallucci, K. Phomphrai, Chem. Commun. (2003) 48–49.
[13] M.H. Chisholm, J. Gallucci, K. Phomphrai, Inorg. Chem. 43 (2004) 6717–6725.
[14] M.H. Chisholm, J. Gallucci, H. Zhen, J.C. Huffman, Inorg. Chem. 40 (2001) 5051–5054.

[15] C.K. Williams, N.R. Brooks, M.A. Hillmyer, W.B. Tolman, Chem. Commun. (2002) 2132–2133.
[16] C.K. Williams, L.E. Breyfogle, S.K. Choi, W. Nam, V.G. Young Jr., M.A. Hillmyer, W.B. Tolman, J. Am. Chem. Soc. 125 (2003) 11350–11359.
[17] L.E. Breyfogle, C.K. Williams, V.G. Young Jr., M.A. Hillmyer, W.B. Tolman, Dalton Trans. (2006) 928–936.
[18] H.Y. Chen, H.Y. Tang, C.C. Lin, Macromolecules 39 (2006) 3745–3752.
[19] D.J. Darensbourg, W. Choi, C.P. Richers, Macromolecules 40 (2007) 3521–3523.
[20] B. Lian, C.M. Thomas, O.L. Casagrande Jr., T. Roisnel, J.-F. Carpentier, Polyhedron 26 (2007) 3817–3824.
[21] B. Lian, C.M. Thomas, O.L. Casagrande Jr., C.W. Lehmann, T. Roisnel, J.-F. Carpentier, Inorg. Chem. 46 (2007) 328–340.
[22] T.R. Jensen, L.E. Breyfogle, M.A. Hillmyer, W.B. Tolman, Chem. Commun. (2004) 2504–2505.
[23] T.R. Jensen, C.P. Schaller, M.A. Hillmyer, W.B. Tolman, J. Organomet. Chem. 690 (2005) 5881–5891.
[24] B.M. Chamberlain, M. Cheng, D.R. Moore, T.M. Ovitt, E.B. Lobkovsky, G.W. Coates, J. Am. Chem. Soc. 123 (2001) 3229–3238.
[25] M.H. Chisholm, J. Gallucci, K. Phomphrai, Inorg. Chem. 41 (2002) 2785–2794.
[26] A.P. Dove, V.C. Gibson, E.L. Marshall, A.J.P. White, D.J. Williams, Dalton Trans. (2004) 570–578.
[27] M.H. Chisholm, J. Gallucci, K. Phomphrai, Inorg. Chem. 44 (2005) 8004–8010.
[28] X. Xu, X.Y. Xu, Y.F. Chen, J. Sun, Organometallics 27 (2008) 758–763.
[29] A.P. Dove, V.C. Gibson, P. Hormnirum, E.L. Marshall, J.A. Segal, A.J.P. White, D.J. Williams, Dalton Trans. (2003) 3088–3097.
[30] A.R. Kennedy, R.E. Mulvey, R.B. Rowlings, J. Organomet. Chem. 648 (2002) 288–292.
[31] Y. Tang, L.N. Zakharov, W.S. Kassel, A.L. Rheingold, R.A. Kemp, Inorg. Chim. Acta 358 (2005) 2014–2022.
[32] A.G. Avent, M.R. Crimmin, M.S. Hill, P.B. Hitchcock, Dalton Trans. (2005) 278–284.
[33] The Mn values obtained from GPC trace using polystyrene standards need to be multiplied by a factor of 0.58 to give the actual Mn of polylactide: J.C. Wu, B.H. Huang, M.L. Hsueh, S.L. Lai, C.C. Lin, Polymer 46 (2005) 9784–9792;
M. Sava, M. Schappacher, A. Soum, Macromol. Chem. Phys. 203 (2002) 889–899.
[34] P_r is the probability of heterotactic enchainment determined by homonuclear decoupled ^{1}H NMR spectroscopy: H.R. Kricheldorf, C. Boettcher, K. -U. Tönnes, Polymer 33 (1992) 2817–2824;
M.T. Zell, B.E. Padden, A.J. Paterick, K.A.M. Thakur, R.T. Kean, M.A. Hillmyer, E.J. Munson, Macromolecules 35 (2002) 7700–7707.
[35] Y. Huang, W.C. Hung, M.Y. Liao, T.E. Tsai, Y.L. Peng, C.C. Lin, J. Polym. Sci., Part A: Polym. Chem. 47 (2009) 2318–2329.
[36] E.H. Amonoo-Neizer, R.A. Shaw, D.O. Skovlin, B.C. Smith, J. Chem. Soc. (1965) 2997–2999.
[37] D.J. Darensbourg, M.W. Holtcamp, G.E. Struck, M.S. Zimmer, S.A. Niezgoda, P. Rainey, J.B. Robertson, J.D. Draper, J.H. Reibenspies, J. Am. Chem. Soc. 121 (1999) 107–116.
[38] G.M. Sheldrick, SADABS, An Empirical Absorption Correction Program for Area Detector Data, University of Goettingen, Germany, 1996.
[39] G.M. Sheldrick, SHELXS-97, University of Goettingen, Germany, 1997.
[40] SMART Version 5.628, Bruker Asx Inc.
[41] SAINT + Version 6.22a, Bruker Axs Inc.
[42] SHELXTL NT/2000, Version 6.1.